Cross Correlating 21 cm Intensity Mapping fields with Kinematic Sunyaev-Zel'dovich Effect: Probing Missing Baryons at $z \sim 1-2$

Dongzi Li,[1,2] Ue-Li Pen,[3,4,5,1] Hong-Ming Zhu,[6,7] and Yu Yu[8]

[1] *Perimeter Institute for Theoretical Physics, 31 Caroline St. N., Waterloo, ON, N2L 2Y5, Canada*
[2] *University of Waterloo, 200 University Ave W, Waterloo, ON, N2L 3G1, Canada*
[3] *Canadian Institute for Theoretical Astrophysics, 60 St. George Street, Toronto, Ontario M5S 3H8, Canada*
[4] *Dunlap Institute for Astronomy and Astrophysics, 50 St. George Street, Toronto, Ontario M5S 3H4, Canada*
[5] *Canadian Institute for Advanced Research, CIFAR Program in Gravitation and Cosmology, Toronto, Ontario M5G 1Z8, Canada*
[6] *Key Laboratory for Computational Astrophysics, National Astronomical Observatories, Chinese Academy of Sciences, 20A Datun Road, Beijing 100012, China*
[7] *University of Chinese Academy of Sciences, Beijing 100049, China*
[8] *Key laboratory for research in galaxies and cosmology, Shanghai Astronomical Observatory, Chinese Academy of Sciences, 80 Nandan Road, Shanghai 200030, China*

(Dated: September 30, 2016)

The obvious defficiency of baryon contents in observations for $z \lesssim 2$ and its close correlation with baryon distributions, galaxy feedbacks and interstellar medium states shed clouds on understanding structure formations. For a comprehensive detection including diffusive baryons, a large scale oriented probe, the kinematic Sunyaev-Zel'dovich (kSZ) effect on cosmic microwave background (CMB), was proposed. However, its faintness and lack of redshift require another signal to cross correlate with it. Previous proposals either require large sky galaxy spectroscopic surveys, or existing photemetric surveys combined with full ACTPol/CMB-S4 data to obtain persuasive results, which is hard to achieve in next five years. In this paper, a new possibility of cross correlating kSZ with HI density from 21cm Intensity Mapping surveys is discussed, Due to the high effeciency and low facility requirements, there are already ongoing experiments like CHIME could satisfy our need. Assuming realistic facility conditions and noise scales, we find that after using nonlinear tidal coupling to retrieve lost information in large scales, a minimum of 15 S/N for both redshift 1 and 2 could be reached with CHIME. With the construction of interferometers with longer baselines such as HIRAX, the S/N could reach 50 for redshift 2.

PACS numbers:

I. INTRODUCTION

For $z \lesssim 2$, large fractions of predicted baryon contents are missing in observations. The majority of them are believed to reside in warm-hot intergalactic mediums (WHIM) with typical temperature of 10^5 K to 10^7 K [1, 2]. High temperature and low density in the medium make us difficult to derive information from metal absroption lines, and uncertainties in ionization states and metalicity will also reduce the reliability. We are looking for signals that not only trace the majority of the baryons, but also easy to interprete.

Among the proposed candidates, the kinematic Sunyaev-Zel'dovich (kSZ) effect [3–5] is a promising one. kSZ effect results from Compton scattering of cosmic microwave background (CMB) off free electrons. The radial velocity of electrons will give photon a Doppler shift and hence leads to a secondary anisotropy in CMB temperature.

KSZ signal is ideal to tackle this problem for three reasons. First, it contributes from all the free electrons, indicating the distribution of 90% of the baryons in ionized states, leaving alone only less than 10% of baryons that reside in stars, remnants, atomic and molecular gases [6]. Second, the signal is mainly influenced by electron density and radial velocity, regardless the temperature, pressure and metalicity, so no extra assumptions are needed to estimate baryon abundance. Third, the peculiar velocity is dominantly related to large scale structures, therefore the signal is less biased towards local mass contraction.

Attractive as it is, two big drawbacks largely reduce the feasibility of harnessing kSZ signal. First, the signal is very weak and hence suffers seriously from contaminations from primary CMB, facility noises, thermal SZ effect, CMB lensing, etc. Second, it is an integrated effect along line of sight, therefore, kSZ itself does not contain redshift information.

A straight-forward mitigation of the two disadvantages is to cross-correlate kSZ signal with another tracer, which has both large scale structure and redshift information. Previous work has proposed optical spectroscopic survey as an ideal tool [7–9]. However, first, it lacks detectable spectral lines in redshift $1.4-2.5$, therefore unable to consistently measure until $z \sim 2$. Moreover we need large sky coverage to compensate for the weakness of kSZ signal, and the low efficiency of spectroscopic survey will make it unaccessible for near future. In this paper we discuss a new possibility for cross correlation—HI density field from 21 cm intensity mapping. HI 21 cm spectra have accurate redshift information, and are fully accessible for $z \lesssim 2$. Intensity mapping is a kind of survey that integrates all the signals in a pixel, rather than distinguishing individual galaxies. It can reach high S/N much faster, hence is very efficient for large sky surveys. There are already several ongoing experiments aim at large sky coverage and claim to be able to reach $z \gtrsim 2$ in very near future, such as CHIME [**?**], Tianlai [10], HIRAX [11] etc.

However, as feasibility is usually traded from data quality, there are three main challenges for the upcoming H I surveys in terms of cross correlation with kSZ. First, the integration of different signals will cause complicated foregrounds, which would smear the large scale structure in radial direction[12, 13]. Second, the angular resolution is also supressed by the integration, droping information of small scale structure in transverse plane. Third, till now, the proposed experiments all work on interferometers, which drain the largest scale structure on transverse plane due to the finite length of the shortest baseline.

On the other hand, the most prominate kSZ signal that could be distinguished from noises contributes mainly from largest structure in radial direction with $l < 100$ and $l \sim 1000$. These modes are seriously damaged in intensity mapping due to the three challenges.

In this paper, we discuss the level of correlation we will get between kSZ and 21cm intensity mappings of different conditions. To lower the requirements on observational experiments, we use a method, cosmic tidal reconstruction [14, 15], to recover some of the large scale structure from its tidal force on small scales.

The paper is organized as follows: In section II, we demonstrate given a density field, how to correlate it with kSZ signal with velocity reconstruction, similar to [8]; we then estimate which modes dominates the produced signal; In section III, we present the result of cross correlation with foreground filtered field, different resolutions, and different shortest baselines and discuss the behavior; Then in section IV, we introduce the method of 3D tidal reconstruction, and present the correlation results after small k modes recovered, In section VI, we estimate statistical error and calculate S/N; and we conclude at section VII.

Notes: Throughout the paper, We use the $z = 1, 2$ output of six N-body simulations from the CUBEP^{3}M code [16], each evolving 1024^3 particles in a $(1.2\mathrm{Gpc}/h)^3$ box. Simulation parameters are as follows: Hubble parameter $h = 0.678$, baryon density $\Omega_b = 0.049$, dark matter density $\Omega_c = 0.259$, amplitude of primordial curvature power spectrum $A_s = 2.139 \times 10^{-9}$ at $k_0 = 0.05\ \mathrm{Mpc}^{-1}$ and scalar spectral index $n_s = 0.968$.

we use "$\wedge$" to denote recontructed fields as oppose to fields directly from simulations.

II. ALGORITHM: KSZ CROSS CORRELATION

In this section, we present a holographic method to cross correlate kSZ with a density field, following [8].

The CMB temperature fluctuations caused by kSZ effect is:

$$\Theta_{kSZ}(\hat{n}) \equiv \frac{\Delta T_{kSZ}}{T_{\mathrm{CMB}}} = -\frac{1}{c}\int d\eta g(\eta)\boldsymbol{p}_{\parallel} , \tag{1}$$

where $\eta(z)$ is the comoving distance at redshift z, $g(\eta) = e^{-\tau} d\tau/d\eta$ is the visibility function, τ is the optical depth to Thomson scattering, $\boldsymbol{p}_{\parallel} = (1+\delta)\boldsymbol{v}_{\parallel}$, with δ the electron overdensity, $\parallel$ indicates direction parallel to line of sight. We assume that $g(\eta)$ doesn't change significally in one redshift bin, and integrate $\boldsymbol{p}_{\parallel}$ along radial axis to get $\hat{\Theta}_{kSZ}$

Due to the cancellation of positive and negative velocity, its direct cross correlation between kSZ signal will vanish. To take advantage of the known redshift and better maintain the one to one multiplication between velocity field and density contrast, we generate a mock kSZ signal from calculation of linear peculiar velocity. In this way, we can at most maximize the correlation.

Assume we have a density contrast field $\delta = (\rho - \bar{\rho})/\bar{\rho}$, where $\bar{\rho}$ is the average density of a certain redshift slice.

Detailed steps are as follows.

(1) Estimate the velocity field:

In linear region, the continuity equation goes like: $\dot{\delta} + \nabla \cdot \boldsymbol{v} = 0$, where $\boldsymbol{v}$ is the peculiar velocity and δ is the matter overdensity.

Therefore, we obtain an estimator of velocity distribution from the density contract δ:

$$\hat{v}_z(\boldsymbol{k}) = iaHf\delta(\boldsymbol{k})\frac{k_z}{k^2} \tag{2}$$

where $f = d\ln D/d\ln a$, $D(a)$ is the linear growth function, a is the scale factor, H is the Hubble parameter.

$v_z \propto k_z/k^2$, indicating the most prominent signal comes from small k mode, which corresponds to large scale structure.

(2) Suppress the noise in velocity field with a Wiener filter. This is because the term k_z/k^2 in Eq.(2) will strongly amplify noises in small k modes.

$$\hat{v}^c_z(\boldsymbol{k}) = \frac{\hat{v}_z(\boldsymbol{k})}{b(k_\perp, k_\parallel)} W(k_\perp, k_\parallel) , \tag{3}$$

Bias $b = P_{\hat{v}_z, v_z}/P_{v_z}$, Wiener filter $W = P_{v_z}/(P_{\hat{v}_z}/b^2)$.

(3) Calculate 2D kSZ map follow Eq.(1).

(4) Calculate correlation coefficients.

We compare reconstructed kSZ signals $\hat{\Theta}_{kSZ}$ with kSZ signals Θ_{kSZ} directly from simulations. To quantify the tightness of correlation, we employ a quantity r:

$$r \equiv \frac{P_{recon,real}}{\sqrt{P_{recon}P_{real}}} \tag{4}$$

III. CONDITION: KSZ + 21CM INTENSITY MAPPING

In this section, we discuss the origin of kSZ signal on different structure scales, and compare it with scales resolvable in ongoing 21cm Intensity Mapping experiments. The main purpose is to give an intuitive picture of the possibility and difficulty of the cross correlation.

A. kSZ properties

To understand what role each scale plays in generating kSZ signal, we write Eq.(1) in Fourier space.

The finite box size of 1200 Mpc will only have obvious influence on modes with $k \lesssim 0.005$, we can safely assume the integration on z direction to be from minus infinity to plus infinity. Moreover, the term $a(z)H(z)f(z)$ in Eq.(2) does not vary much in one box, we assume it to be a constant for

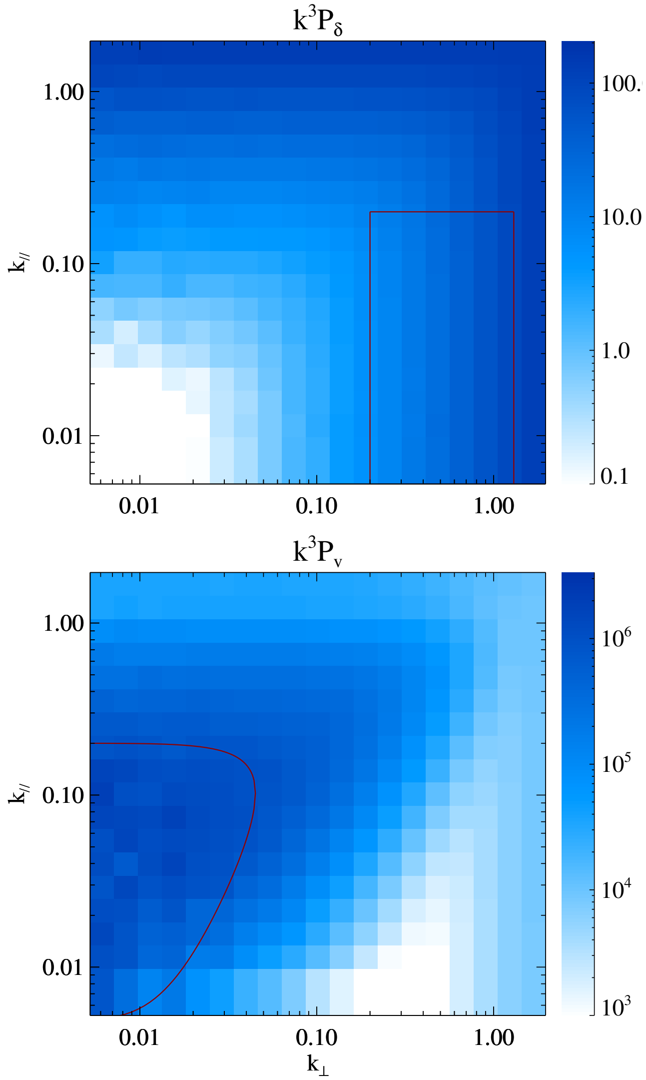

FIG. 1: Illustrating weights of different scales after integration for redshift 1. (Top) The density variance $2\pi^2\Delta^2_\delta \equiv k^3 P_\delta$. (Bottom) The velocity variance $2\pi^2\Delta^2_{v_z} \equiv k^3 P_{v_z}$. Red lines: indicate the most essential modes for generating kSZ signal in ℓ $500-3000$.

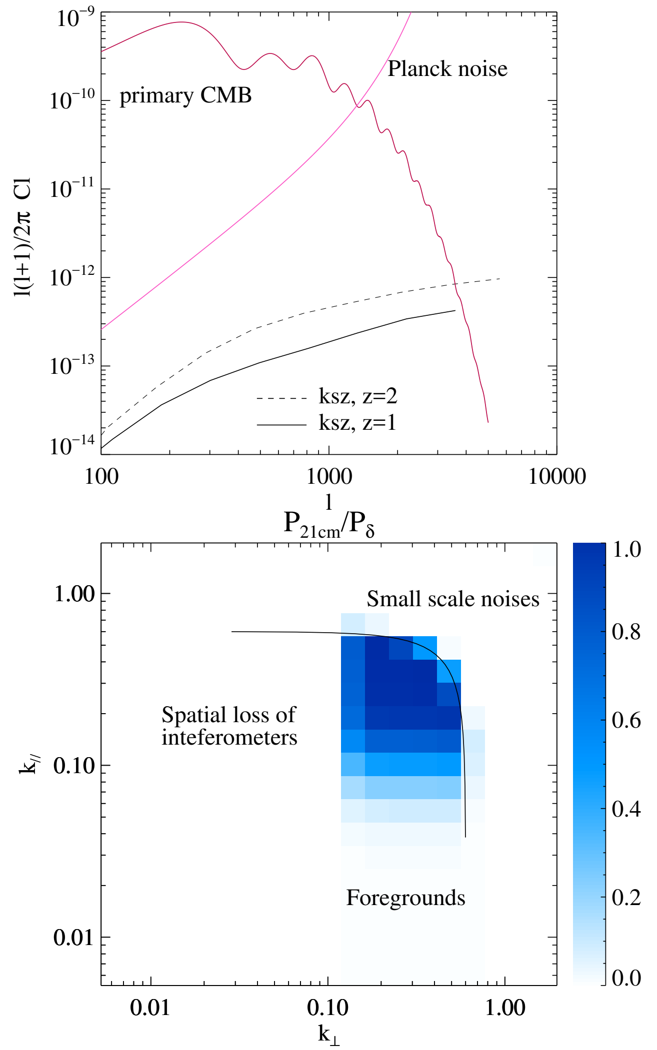

FIG. 2: (Top) Relative strength of angular powerspectrum between primary CMB, Planck noise in 217 GHz band, and kSZ effect in redshift 1 and 2. (Bottom) Demonstrate available modes of density contrasts obtained in realistic 21cm Intensity Mapping experiments. P_{21cm} is the remaining density powerspectrum after noise substraction; P_δ indicates the powerspectrum of a comtact density field.

simplicity. Then the Fourier transformation is just the $k_z = 0$ mode of the momentum $p_\parallel(\boldsymbol{k})$ in Fourier space.

$$\Theta(\boldsymbol{l}) \equiv \Theta \ \ (k_x\chi, k_y\chi, 0) \propto \int d^3k' \delta(\boldsymbol{l}/\chi - \boldsymbol{k}'_\perp, k'_\parallel) v_z(\boldsymbol{k}') \tag{5}$$

An essential feature of Eq.(5) is that in transverse plane, density and velocity field of different scales are multiplied together; while in parallel direction, only δ and v_z with identical k_z are coupled together.

The relative strength of $|\delta(\boldsymbol{k})|$ and $|v_z(\boldsymbol{k})|$ in different scales are implied in Fig.1. It is obvious that the velocity field contributes almost dominantly from large scale structures, leaving little contribution from $k_z > 0.2h/Mpc$ with $k_\perp > 0.02h/Mpc$. This makes it roughly an ellipitical selection functions in the convolution — It selects δ with similar range of k_z and $k_\perp \sim l/\chi - 0.01$ h/Mpc. To see it clearly, let us assume that $|v(\boldsymbol{k})|$ drops fast enough for large k and could be demonstrated as a Delta Function centered at $(k_\perp, k_\parallel) = (0.01, 0.1)$ h/Mpc. then it is immediately shown that

$$\Theta(\boldsymbol{l}) \ \propto \int d^3k' \delta(\boldsymbol{l}/\chi - \boldsymbol{k}'_\perp, k'_\parallel) \delta^D(0.01, 0.1) \tag{6}$$

$$\sim \delta(\boldsymbol{l}/\chi - 0.01, 0.1). \tag{7}$$

Therefore, when generating kSZ signals, it is crucial to have large scale modes for v_z. However, which scale matters most for $\delta(\boldsymbol{k})$ depends on the ℓ we look at.

To decide the targeted ℓ range, there are many factors to consider: the strength of the primary CMB, facility limits and other fluctuations on CMB such as thermal SZ effect**??**

and CMB lensing**??**. Consider using Plank**??** data in the 217 GHz band, where the tSZ signal vanishes, we demonstrate the angular powerspectrum of primary CMB, facility noises, and kSZ of redshift 1 and 2. As shown in Fig.**??**, only in the range of $\ell \sim 500 - 3000$, there is a chance for us to distinguish the kSZ signal.

In Fig.1, we demonstrate the essential modes for mock kSZ signal in both $v_z(\boldsymbol{k})$ and $\delta(\boldsymbol{k})$ fields with red lines. Linearly, velocity field of a certain scale only relates to identical scale of density field, see Eq.(2). Therefore, an ideal cross correlation density field should be comtact in both regions.

Note: all the demonstration figures are towards redshift 1, however there is no distinctive difference for quantitive analysis at redshift 2.

B. 21 cm Intensity Mapping Properties

Main drawbacks of ongoing 21cm Intensity Mapping experiments are demonstrated with simple filters.

1. Small scale noises:

The finite spacial and velocity resolution of facilities prevent us from resolving infinitely small structures in both parallel and perpendicular directions. Therefore we import a cut off scale k_{max} with a Heaviside Function $H(k_{max} - k)$, dropping all the modes with k larger than k_{max}.

2. Foreground noises:

Foregrounds coming from Galactic emissions, telescope noise, extragalactic radio sources and Radio recombination lines, could be three orders brighter than actual signals[12, 13]. The process of foreground removal, taking advantage of its low spectral degrees of freedom [17], will inevitably contaminates the smooth large scale structure in radial direction. To imitate the loss, a high pass filter $W_{fs}(k_\parallel) = 1 - e^{-k_\parallel^2 R_\parallel^2/2}$ is applied to density contraction.

3. Spatial loss of inteferometers:

Large scale structure in perpendicular plane, due to the smoothness, will appear sharp in the visibility function of interferometers after Fourier Transformation. Unfortunately that sharp peak could not be resolved by interferometers due to the incomplete sampling caused by the finite length of the shortest baselines. Therefore, structures with angular sizes greater than a threshold l_{min} are assumed to be lost in our simulations.

In sum, the observed 21 cm density contrasts after all the loss will appear as

$$\delta_{nf}(\boldsymbol{k}) = \delta(\boldsymbol{k}) H(k_{max} - k) W_{fs}(k_\parallel) H(l - l_{min}), \quad (8)$$

The chosen parameters and reasons are presented in Table. I.

The demonstration of a worst case for $z = 1$ is shown in Fig.**??**. As we could see, essential modes for density field are partly resolved. However, the reconstruction of velocity field will be a total failure due to the spatial loss of inteferometers.

If we directly use this density contrast to generate mock kSZ signal, its correlation r (Eq.(**??**)) with real kSZ will be at most 0.2. Luckily, till now we only use the linear theory for reconstruction, while nonlinearly modes of different scales are coupled. If we could identify a relatively clean nonlinear effect in density field, we would be able to retrieve the information needed for velocity reconstruction. The effect we choose is the tidal influence of large scale structure on small scales, following [14, 15].

	z=1		z=2	
	high foreground	low foreground	high foreground	low foreground
[a] $R_\parallel$ Mpc/h	15	60	10	40
	CHIME	HIRAX	CHIME	HIRAX
[b] k_{max} h/Mpc	0.6	1.2	0.4	0.8
[c] ℓ_{min}	300			

[a]Foreground: smear $k_z \lesssim 0.08, 0.02, 0.12, 0.03$ h/Mpc respectively. Parameters based on [18–20]
[b]Small scale noises: based on CHIME[21] and HIRAX[11] with 100 m and 200 m longest baseline respectively.
[c]Spatial loss of inteferomenter: assuming shortest baseline of 20 m.

TABLE I: Parameter of different noise filtering.

IV. ALGORITHM: COSMIC TIDAL RECONSTRUCTION

The evolution of small scale structure is modulated by large scale gravitational force. We can select this effect and solve for the large scale potential.

Consider only the anisotropic influence from tidal force, the distortions on power spectrum can linearly be calculated as

$$\delta P(\boldsymbol{k}, \tau)|_{t_{ij}} = \hat{k}^i \hat{k}^j t_{ij}^{(0)} P_{1s}(k, \tau) f(k, \tau) \quad (9)$$

where f is the linear coupling function; $P_{1s}(k, \tau)$ is the theoretical small scale linear powerspectrum; and $\delta P(\boldsymbol{k}, \tau)$ is the real distortion from observations.

Hence we can solve for the unknown quantity t_{ij}, which is the tidal force tensor defined as

$$t_{ij} = \Phi_{L,ij} - \nabla^2 \Phi_L \delta_{ij}^D / 3 \quad (10)$$

$\Phi_{L,ij}$ is the second derivative of large scale potential, δ^D is the Dirac function.

With t_{ij}, we calculate the variance of large scale potential Φ_L and get the large scale density contrast $\kappa_{3\mathrm{D}}$.

$$\kappa_{3\mathrm{D}} \sim \nabla^2 \Phi_L = \frac{3}{2} \nabla^{-2} \partial_i \partial_j t_{ij} \quad (11)$$

Since $f(k, \tau)$ increase with k in our interested scales, the distortions are more obvious in small scales. Therefore, the method mainly use the quadratic statistics on small scales to recover the large scale density field. It works best for close linear regions.

Programming steps:

(1) Gaussianize the field, taking $\delta_g = \ln(1 + \delta)$. This is to allieviate the problem that filter W_i in Eq.(14) heavily weights high density regions.

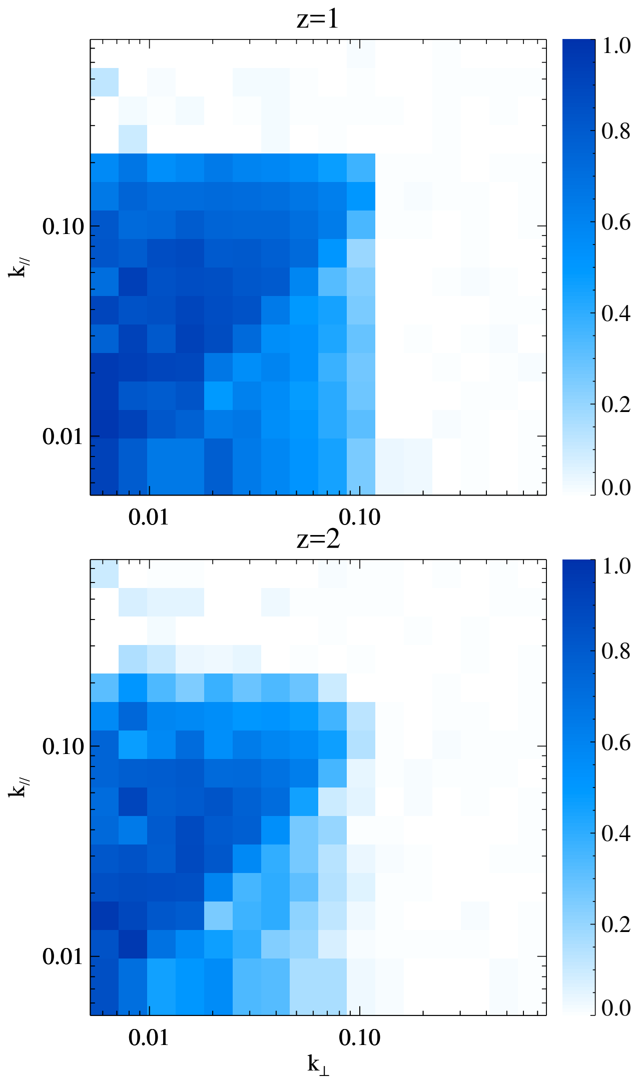

FIG. 3: Cross correlation r of reconstructed velocity field with real velocity field, assuming a baseline of 100m and serious foregrounds below k_z 0.08 h/Mpc and 0.12 h/Mpc for redshift 1 and 2 respectively.

(2) Following gravitational lensing procedures, decompose the symmetric, traceless tidal force tensor into 5 components,

$$t_{ij} = \begin{pmatrix} \gamma_1 - \gamma_z & \gamma_\times & \gamma_2 \\ \gamma_\times & -\gamma_1 - \gamma_z & \gamma_y \\ \gamma_2 & \gamma_y & 2\gamma_z \end{pmatrix}. \quad (12)$$

(3) Select density distortions caused by tidal force, by convolving δ_g with a filter W_i deduced from Eq.(9)

$$\delta_g^{w_i}(\boldsymbol{k}) = W_i(\boldsymbol{k})\delta_g(\boldsymbol{k}) \quad (13)$$

$$W_i(\boldsymbol{k}) = i\left[\frac{P(k)f(k)}{P_{tot}^2(k)}\right]^{\frac{1}{2}}\frac{k_i}{k} = S(k)\frac{k_i}{k}$$

where i indicates $\hat{x}, \hat{y}, \hat{z}$ directions, $f(k) = 2\alpha(\tau) - \beta(\tau)d\ln P/d\ln k$ is again the coupling function, with α and β related to linear growth funcion [15], and calculated to be (0.6, 1.3) for $z = 1$ and (0.4, 0.9) for $z = 2$. $P_{tot} = P + P_{noise}$ is observed matter powerspectrum, P is theoretical matter powerspectrum,

(4) Estimate the 5 tidal tensor components from quadratic statistics.

$$\begin{aligned}
\hat{\gamma}_1(\boldsymbol{x}) &= [\delta_g^{w_1}(\boldsymbol{x})\delta_g^{w_1}(\boldsymbol{x}) - \delta_g^{w_2}(\boldsymbol{x})\delta_g^{w_2}(\boldsymbol{x})], \\
\hat{\gamma}_2(\boldsymbol{x}) &= [2\delta_g^{w_1}(\boldsymbol{x})\delta_g^{w_2}(\boldsymbol{x})], \\
\hat{\gamma}_x(\boldsymbol{x}) &= [2\delta_g^{w_1}(\boldsymbol{x})\delta_g^{w_3}(\boldsymbol{x})], \\
\hat{\gamma}_y(\boldsymbol{x}) &= [2\delta_g^{w_2}(\boldsymbol{x})\delta_g^{w_3}(\boldsymbol{x})], \\
\hat{\gamma}_z(\boldsymbol{x}) &= \frac{1}{3}[(2\delta_g^{w_3}(\boldsymbol{x})\delta_g^{w_3}(\boldsymbol{x}) \\
&\quad -\delta_g^{w_1}(\boldsymbol{x})\delta_g^{w_1}(\boldsymbol{x}) - \delta_g^{w_2}(\boldsymbol{x})\delta_g^{w_2}(\boldsymbol{x}))],
\end{aligned} \quad (14)$$

(5) Reconstruct large scale density contrast $\kappa_{3\mathrm{D}}$ from tidal tensor:

$$\begin{aligned}
\kappa_{3\mathrm{D}}(\boldsymbol{k}) = \frac{1}{k^2} \quad & [(k_1^2 - k_2^2)\gamma_1(\boldsymbol{k}) + 2k_1k_2\gamma_2(\boldsymbol{k}) \\
& +2k_1k_3\gamma_x(\boldsymbol{k}) + 2k_2k_3\gamma_y(\boldsymbol{k}) \\
& +(2k_3^2 - k_1^2 - k_1^2)\gamma_z(\boldsymbol{k})].
\end{aligned} \quad (15)$$

(6) Correct bias and suppress noise with a Wiener filter.

Due to the foregrounds, the noise in z direction will be different from x,y direction, therefore we apply an anisotropic Wiener filter.

$$\hat{\kappa}_c(\boldsymbol{k}) = \frac{\kappa_{3\mathrm{D}}(\boldsymbol{k})}{b(k_\perp, k_\parallel)}W(k_\perp, k_\parallel)\,, \quad (16)$$

Bias $b(k_\perp, k_\parallel) = P_{\mathrm{k3D},\delta}/P_\delta$ is the cross powerspectra between reconstructed field κ3D and original field δ, Wiener filter $W(k_\perp, k_\parallel) = P_\delta/(P_{\mathrm{k3D}}/b^2)$.

Here $\hat{\kappa}_c$ is the output large scale density contrast we obtain from tidal reconstruction. We use it to calculate velocity $\hat{v}_z^{\mathrm{tide}}$.

V. RESULTS

To avoid manipulating noises, we perform tidal reconstruction on most conservative estimates, i.e. $R_\parallel = 15$ Mpc/h, $k_{max} = 0.6$ h/Mpc, $\ell_{max} = 100$ for $z = 1$; $R_\parallel = 10$ Mpc/h, $k_{max} = 0.4$ h/Mpc, $\ell_{max} = 100$ for $z = 2$.

The cross correlation between $\hat{v}_z^{tide}$ and v_z are demonstrated in Fig.3. Important modes for velocity fields(within redline of Fig.**??** lower label) are well extracted with correlation greater than 0.7. The reconstruction on $z = 2$ is slightly worse than $z = 1$ due to stronger foreground and lower resolution.

Combining reconstructed velocity field with density fields of different conditions, we get mock kSZ signals. Their correlation coefficients with exact kSZ are demonstrated in Fig.4. Even with identical tidal reconstructed velocity field, better foreground techneque can improve the correlation coefficient by 0.2. If the foreground is removed clean enough for more modes to be used in tidal reconstruction procedure, the improvement will be more notable. Resolution of facility will improve the reconstruction on higher ℓ, consisting with previous analysis.

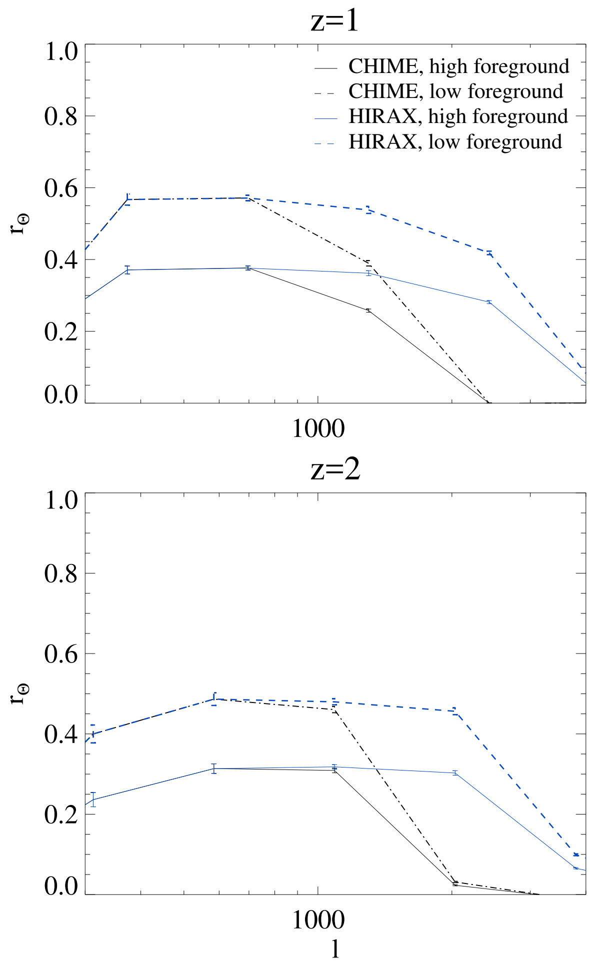

FIG. 4: The cross correlation r between real kSZ $P_{\Theta_{kSZ}}$ and reconstructed kSZ $P_{\hat{\Theta}_{kSZ}}$.

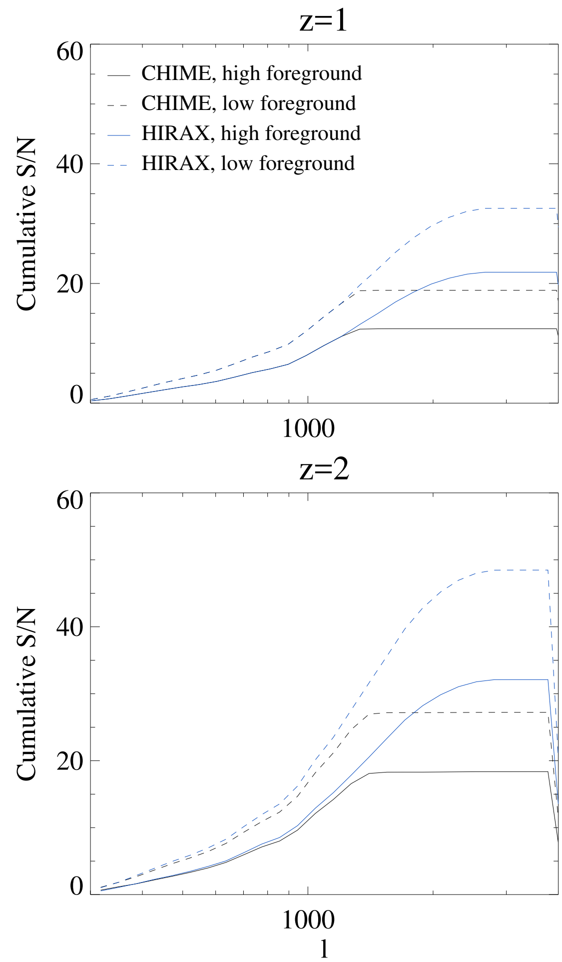

FIG. 5: Accumulative S/N, assuming Planck noise at 217 GHz, $f_{sky} = 0.8$.

VI. STATISTICAL ERROR AND S/N

Taking into account primary CMB and facility noises, the chance to seperate kSZ signal from statistical errors could be estimated as

$$\begin{aligned} \frac{S}{N} &= \frac{C_l}{\Delta C_l} \qquad (17) \\ &\simeq r\sqrt{(2\ell+1)\Delta l f_{\rm sky}}\sqrt{\frac{C_l^{\rm kSZ,\Delta z}}{C_l^{\rm CMB}+C_l^{\rm kSZ}+C_l^{{\rm CMB},N}}} \end{aligned}$$

Where $C_l^{\rm CMB}$ is the angular powerspectrum of primary CMB ; $C_l^{\rm CMB,N}$ indicates the facility noises; $C_l^{\rm kSZ,\Delta z}$ is the kSZ signal from a certain redshift bin; r is the correlation coefficients we get; $f_{\rm sky}$ is the percent of sky area covered by both surveys.

In our case, $C_l^{\rm CMB}$ is calculated from CAMB [22]. $C_l^{\rm CMB,N}$ is estimated with Planck results [23] at 217GHz. $C_l^{\rm CMB,N} = (\sigma_{p,T}\theta_{\rm FWHM})^2 W_l^{-2}$; where $\sigma_{p,T} = 8.7\mu K_{\rm CMB}$ is Sensitivity per beam solid angle, $\theta_{\rm FWHM} \sim 5'$ is the effective beam FWHM, $W_l = \exp[-\ell(\ell+1)/2\ell^2_{\rm beam}]$ is the smoothing window function, with $\ell_{\rm beam} = \sqrt{8\ln 2}/\theta_{\rm FWHM}$. We choose $f_{\rm sky} = 0.8$ according to claimed 21 cm intensity mapping survey area. $C_l^{\rm kSZ,\Delta z}$ is calculated within two bins of size 1200 Mpc/h, centered at redshift 1,2 respectively.

The cumulative S/N is demonstrated in Fig.5. The low correlation in $z = 2$ is compensated by the high electron density and the overall S/N could well reach 50 with HIRAX.

With noise level of Planck, the resolution of HIRAX already cover most important ℓs. However, with $4_{\rm th}$ generation facilities, more detectable modes will apprear in higher ℓs, and better S/N could be expected with longer baselines like SKA.

VII. CONCLUSION

In this paper, we discuss the possibility of cross correlating kSZ signal with 21 cm intensity mapping to study baryon distributions. All the calculations are based on ongoing experiment condition and realistic noise scales. A holographic way of cross correlation is applied. Second order tidal coupling of different scales are employed to compensate for lost modes. With existing Planck data, it is reasonable to expect at least 15 S/N with data from CHIME, and more optimistic estimates will yield 50 S/N for redshift 2 with HIRAX. The main obstacle for optimal correlation is lack of low k_z high $k_\perp$ data due to foregrounds. This leads to information waste in the reconstructed velocity field. However, data from weak lensing, photometric galaxy surveys, which contains only large scale structure in z direction, may compensate for that.

This method is promising for its feasibility and model independence. CHIME has already started to collecting data, and HIRAX is also in a close flight. It is reasonable to expect it to be tested within five years. Moreover, the method does not rely on assumptions about velocity fields or interstellar medium conditions. Less misunderstanding will appear in interpreting results. It is reasonable to expect it to be a new reliable attemp to study baryon distributions up to redshift 2 or higher. This will foster the understanding of baryonic feedbacks of galaxies, and the condition in ISM.

VIII. ACKNOWLEDGE

We acknowledge discussions with Kendrick Smith, Matthew Johnson, Wenkai Hu, Tianxiang Mao and Jiawei Shao. The simulations were performed on the BGQ supercomputer at the SciNet HPC Consortium. SciNet is funded by: the Canada Foundation for Innovation under the auspices of Compute Canada; the Government of Ontario; the Ontario Research Fund – Research Excellence; and the University of Toronto. Research at the Perimeter Institute is supported by the Government of Canada through Industry Canada and by the Province of Ontario through the Ministry of Research & Innovation. The Dunlap Institute is funded through an endowment established by the David Dunlap family and the University of Toronto.

[1] U.-L. Pen, ApJ **510**, L1 (1999), astro-ph/9811045.
[2] A. M. Sołtan, A&A **460**, 59 (2006), astro-ph/0604465.
[3] R. A. Sunyaev and Y. B. Zeldovich, Comments on Astrophysics and Space Physics **4**, 173 (1972).
[4] R. A. Sunyaev and I. B. Zeldovich, MNRAS **190**, 413 (1980).
[5] E. T. Vishniac, ApJ **322**, 597 (1987).
[6] M. Fukugita and P. J. E. Peebles, ApJ **616**, 643 (2004), astro-ph/0406095.
[7] N. Hand, G. E. Addison, E. Aubourg, N. Battaglia, E. S. Battistelli, D. Bizyaev, J. R. Bond, H. Brewington, J. Brinkmann, B. R. Brown, et al., Physical Review Letters **109**, 041101 (2012), 1203.4219.
[8] J. Shao, P. Zhang, W. Lin, Y. Jing, and J. Pan, MNRAS **413**, 628 (2011), 1004.1301.
[9] M. Li, R. E. Angulo, S. D. M. White, and J. Jasche, MNRAS **443**, 2311 (2014), 1404.0007.
[10] Y. Xu, X. Wang, and X. Chen, ApJ **798**, 40 (2015), 1410.7794.
[11] http://www.acru.ukzn.ac.za/ hirax/.
[12] T. Di Matteo, B. Ciardi, and F. Miniati, MNRAS **355**, 1053 (2004), astro-ph/0402322.
[13] K. W. Masui, E. R. Switzer, N. Banavar, K. Bandura, C. Blake, L.-M. Calin, T.-C. Chang, X. Chen, Y.-C. Li, Y.-W. Liao, et al., ApJ **763**, L20 (2013), 1208.0331.
[14] U.-L. Pen, R. Sheth, J. Harnois-Deraps, X. Chen, and Z. Li, ArXiv e-prints (2012), 1202.5804.
[15] H.-M. Zhu, U.-L. Pen, Y. Yu, X. Er, and X. Chen, ArXiv e-prints (2015), 1511.04680.
[16] J. Harnois-Déraps, U.-L. Pen, I. T. Iliev, H. Merz, J. D. Emberson, and V. Desjacques, MNRAS **436**, 540 (2013), 1208.5098.
[17] E. R. Switzer, T.-C. Chang, K. W. Masui, U.-L. Pen, and T. C. Voytek, ApJ **815**, 51 (2015), 1504.07527.
[18] K. W. Masui, E. R. Switzer, N. Banavar, K. Bandura, C. Blake, L.-M. Calin, T.-C. Chang, X. Chen, Y.-C. Li, Y.-W. Liao, et al., ApJ **763**, L20 (2013), 1208.0331.
[19] E. R. Switzer, K. W. Masui, K. Bandura, L.-M. Calin, T.-C. Chang, X.-L. Chen, Y.-C. Li, Y.-W. Liao, A. Natarajan, U.-L. Pen, et al., MNRAS **434**, L46 (2013), 1304.3712.
[20] J. R. Shaw, K. Sigurdson, M. Sitwell, A. Stebbins, and U.-L. Pen, Phys. Rev. D **91**, 083514 (2015), 1401.2095.
[21] K. Bandura, G. E. Addison, M. Amiri, J. R. Bond, D. Campbell-Wilson, L. Connor, J.-F. Cliche, G. Davis, M. Deng, N. Denman, et al., in *Society of Photo-Optical Instrumentation Engineers (SPIE) Conference Series* (2014), vol. 9145 of *Society of Photo-Optical Instrumentation Engineers (SPIE) Conference Series*, p. 22, 1406.2288.
[22] A. Lewis, A. Challinor, and A. Lasenby, Astrophys. J. **538**, 473 (2000), astro-ph/9911177.
[23] Planck Collaboration, R. Adam, P. A. R. Ade, N. Aghanim, M. Arnaud, M. Ashdown, J. Aumont, C. Baccigalupi, A. J. Banday, R. B. Barreiro, et al., ArXiv e-prints (2015), 1502.01587.